Numerical investigation of Magneto hydrodynamics effects on natural silver nanoparticles from *Sargassum angustifolium* used for transporting a pharmaceutical compound in *Cyprinus carpio*

M. Y. Abdollahzadeh Jamalabadi[1*] and A. J. Keikha[2]

[1]*Department of Mechanical, Robotics and Energy Engineering, Dongguk University-Seoul Seoul, 04620, Korea*
[2]*Chabahar Maritime University, Chabahar 99717-56499, Iran*
Corresponding Email: muhammad_yaghoob@yahoo.com

_____

ABSTRACT

In this study, the effect of high flux magnetic field on silver nanoparticles under its acute toxicity produced by seaweed Sargassum angustifolium that is produced by biological methods were investigated. The produced nanoparticle by natural method can have reached the average size of the bio nanoparticles of 102 nm with spherical form. Since the lethal concentration of LC50 was found to be less than one mili-mole per liter for common carp, the lower concentration was used in numerical study. Magnetic nanoparticles suspended in non-Newtonian bio-fluids (blood) as drug carrier are widely used in industries and medicines as magnetic separation tool, anti-cancer drug carrier, micro valve application in micro channels and etc. The governing non-linear differential equations, concentration and Naviar-stokes are coupled with Maxwell's magnetic field. The coupling of magnetic force, fluid velocity, drag forces and diffusion coefficient with concentration makes the problem very tedious. To solve these equations, a finite volume based code with SIMPLE scheme is developed and utilized. Results show accumulation of magnetic Nano-particles near the magnetic source. As time passes the accumulation increases until it looks like a solid object. This is attributable to the compromise flanked by the magnetic and fluid drag forces. As magnetic effect and size of magnetic particles increases the amassing close to the source increases as well. As well the magnetic susceptibility of particles affects the flow field andcontour of concentration considerably.

Keywords: magnetohydrodynamics, silver nanoparticles, seaweed, common carp
_____

INTRODUCTION

In recent decades, progression of nano-technology [1-4], many theoretical phenomena have originated their reputation in emerging applications [5-10]. Targeted drug delivery by using magnetic nanoparticles is an efficient technique to deliver drug molecules to specific tissues in an animal [11-15]. An electromagnetic actuation system is a promising solution for applying an adequate force to direct the magnetic nanoparticles in the blood vessels in a noninvasive way [16-25]. To do that a combined actuation and monitoring system is required to provide a closed-loop nanoparticle localization of the magnetic nanoparticles on the basis of magnetic particle imaging for more precise targeting [26-30]. The magnetic nanoparticles can be navigated by applying a magnetic field gradient provided by the actuation system and monitored by applying the drive and selection fields to the actuation coils by using a time division multiplexing scheme [31-35]. Between various nanoparticle types, the silver nanoparticles (AgNps) are extensively investigated because of wide range applications such as antibacterial, catalyst, medical devices, photonics, optoelectronics and biosensors [36-37]. Usually metallic nanoparticles are synthesized by chemical, mechanical and electrochemical methods [38]. In these methods for the synthesis of silver nanoparticles used toxic chemicals compounds that can have negative effects on the environment and water ecosystems. To investigate the feasibility of combining the actuation system an MPI system is required which used an efficient numerical simulations and optimizing hardware constraints. The challenge of that aim is to sequence the actuation signal and the MPI signal to perform both tasks simultaneously. The simulation results showed the feasibility of the MPI-based actuation system. The proposed system will provide simultaneous navigation and tracking for targeted drug delivery of MNPs in compact and efficient ways. As a result of the devastating effects of these methods on the

52

marine environment, at present several methods for the synthesis of these nanomaterials are necessary. One of these methods that's more compatible with the environment and create less pollution, are biological methods. In this method to synthesis metal nanoparticles, used microorganism and plant materials that exist in nature instead of toxic chemicals [39]. One of the resources that can be used in nanotechnology and synthesis of nanoparticles are seaweeds that have variety types of phytochemical compounds such as proteins, carbohydrates, alkaloids, steroids, phenols, saponins and flavonoids [40] play key role in bio reduction of the metal ions into Nano form. Toxicity of silver ion has been known for centuries but silver nanoparticles toxicity may be dependent on particle concentration, particle size and shape and surface chemistry [41]. In recent years, several studies have been conducted regarding to the effect of silver nanoparticles synthesized by chemical methods on fish toxicity [42-45]. Through the literature search [46-63], no researches have studied the applicability of using Ag nanoparticles for drug delivery in animals. Magnetic drug targeting is a drug delivery approach in which therapeutic magnetizable particles are injected, generally into blood vessels, and magnets are then used to guide and concentrate them in the diseased target organ. Previous study [63] done by author and cooperators is the first study on the toxicity of silver nanoparticles synthesized using biological methods on common carp. The purpose of this study is feasibility study of magnetic effects on silver nanoparticles for drug and gene delivery in fishes. The present invention provides a two-dimensional analysis using differential equations of fluid flow for the purpose of delivering magnetic nanoparticles.

MATERIALS AND METHODS

The applicability of the current study requires a drive device which is adapted such that particle magnetization and electromagnetic field gradient can be simultaneously satisfied by using a DCC system, and is adapted such that the overall three-dimensional drive unit size can be minimized by reducing the number of coils and current-supply units, and is able to generate a high electromagnetic field gradient and a high particle drive force by inserting cores in the centers of the coils and thereby concentrating the electromagnetic field. Figure 1 depicts the schematic of the flux density distribution on a blood artery. The coil is in the X-Y plane and Magnetic Field is evaluated. The flow is 2-dimensioanl, laminar and non-Newtonian. A permanent magnet is placed over the top wall of the channel. The center of this permanent magnet is located at 3mm from the top wall of the vessel, see Figure 1. The external permanent magnetic field is applied vertically with it intensity at the center equal to 10^6 A/m and its diameter equal to 4mm, as shown by Figure 1.
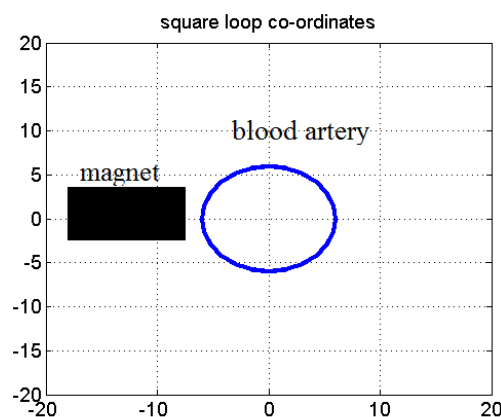

Fig.1. Position of Magnet to apply on blood artery

Here the drug delivery from the body to the cellular scale in animal and human clinical trials is studied by magnetic resonance (MR) image for a cancer patient where magnetic nano-particle accumulate as lighter regions at the arrow tips (due to the MR extinction phenomena). Magneto-particle can concentrated in rabbit tumor micro-vessels or at the membrane of mouse epithelial cells.

Governing equations including for bio-fluid, blood with magnetic Nano-particles, in x and y direction are as follows:

$$\rho \left(u \frac{\partial u}{\partial x} + v \frac{\partial u}{\partial y} \right) = -\frac{\partial P}{\partial x} + \mu \left(\frac{\partial^2 u}{\partial x^2} + \frac{\partial^2 u}{\partial y^2} \right) + F_x \tag{1}$$

$$\rho \left(u \frac{\partial v}{\partial x} + v \frac{\partial v}{\partial y} \right) = -\frac{\partial P}{\partial y} + \mu \left(\frac{\partial^2 v}{\partial x^2} + \frac{\partial^2 v}{\partial y^2} \right) + F_y \tag{2}$$

Where F_x and F_y represent the effect of magnetic particles concentration on fluid in x and y direction, respectively. The nanoparticles can obtain with the method of Abdollahzadeh et al. [63]. After adding silver nitrate to *Sargassum*

anustifolium extract, the brownish-yellow color in mixture turned in to dark brown color after 110 min (Fig 1). To make sure the synthesis of silver nanoparticles, nanoparticle absorption peak was measured using UV-visible spectrometer (UV-Vis) in the wavelength range of 200-700 nm. The best peak was observed after 2h of reaction time in the range of 406 nm, which corresponds to plasmon excitation of the AgNPs. The peak formed in this range represented reduction of silver ions and after synthesis of silver nanoparticles using extracts of seaweed Sargassum. TheUV-Vis absorption spectrum of silver nanoparticles synthesized by treating 1mM AgNO3 solution with *Sargassum anustifolium* extract [63].According to the TEM analysis, average size of synthesized silver nanoparticles was 32.54nm and predominately spherical in shape (Fig 2).
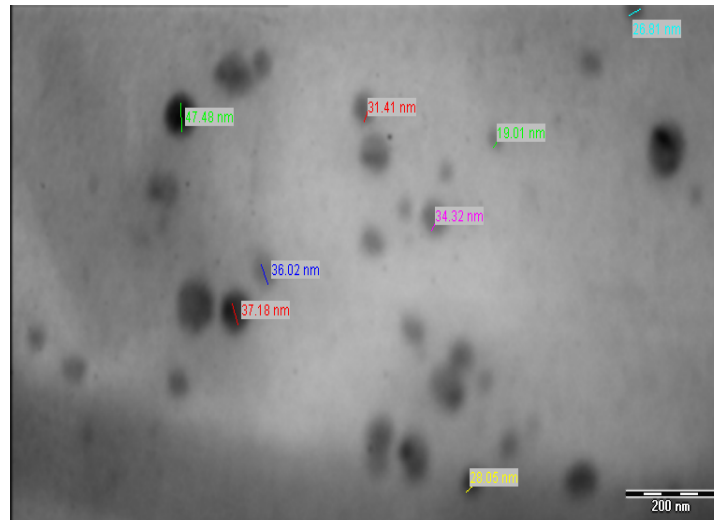

Fig. 2.TEM images of AgNPs synthesized by *Sargassum anustifolium*[63]

As shown in [63], apart from the perfect spherical shape and size all particles dispersion was good and well–distributed in solution and is not in contact with each other. The viscous, steady, two-dimensional, incompressible, laminar biomagnetic fluid (blood) flow is considered as taking place through a forked artery with a stenosis. The flow is subject to a magnetic source, which is located very close to the lower wall and below it. The flow at the entrance is expected to be fully developed and all the arterial walls are kept at a constant temperature, while the fluid is higher than wall. The origin of the Cartesian coordinate system is located at the leading edge of the lower wall. The volume force terms (F_x and F_y) are equal to the magnetic forces on a single particle at that location multiplied by the number of particles per unit volume by, n ($F_x = nF_{Mag-x}$). The magnetic force on single particle and F_x and F_y are as follows, respectively. The magnetophoretic force (FMAP) depends on the gradient of the magnetic intensity and the effective magnetic dipole moment (Meff) of the particles. It can be expressed as:

$$F_{Mag} = \frac{1}{2} (Volume)_P \mu_0 \chi \nabla H^2 \tag{3}$$

$$F_x = \left[\frac{1}{2} \mu_0 \chi \frac{\partial}{\partial x} (\vec{H}.\vec{H})\right] C_V \tag{4}$$

$$F_y = \left[\frac{1}{2} \mu_0 \chi \frac{\partial}{\partial y} (\vec{H}.\vec{H})\right] C_V \tag{5}$$

Considering, the nano-particle as a homogeneous sphere with radius R and netmagnetic polarization M that is suspended in a magnetically linear fluid of permeability and subjected to a magnetic intensity. Magnetizable materials exhibit strong non-linear behavior, such as paramagnets and ferromagnetism, which cannot beignored when modeling the electro mechanics of magnetic particles. Materials with non-linear magnetic properties can be divided into hard and soft materials. For both, magnetization is related to the magnetic intensity, although for hard materials, it also depends on the history of magnetization, which is termed hysteresis. The principal manifestation of non-linearity in magnetic materials is *saturation*, which limits the magnitude of the magnetization vector to a finite value. The influence of saturation on the effective moment of a particle is evident.

Blood is considered to be an electrically conducting bio magnetic Newtonian fluid and is assumed to be Newtonian, since there is a very little variation of viscosity with the applied magnetic field. Although blood is suspension of particles and should be treated as a non-Newtonian flow, it is generally accepted that it behaves as a Newtonian flow in arteries with large diameters. Likewise, the rotational forces acting on the erythrocytes when entering and exiting the magnetic field are discarded (equilibrium magnetization). The walls of the channel are assumed electrically non-

54

conducting and the electric field is considered negligible. Where in Eqs (4) and (5) C_V is volume concentration (number of particles per unit volume) and is as follow:

$$C_V = C_{V0}C \tag{6}$$

Where C_{V0} is initial volume concentration that equal to 0.03 and non-dimensional volume concentration (C) is determined by [8]:

$$\frac{\partial C}{\partial t} + \nabla.\left(Cv_p\right) = \nabla.(D\nabla C) \tag{7}$$

The magnetization process of red blood cell behaves like the following function, known as the Langevin function, which defines the variation of magnetization with magnetic field. In equation (7) velocity of particles, v_p is calculated by balancing the hydrodynamic and magnetic forces and is given by Stokes drag law [8]:

$$\left(v_P = v_f + v_{MAG}\right) \tag{8}$$

Where:
$$v_{Mag} = \frac{F_{Mag}}{6\pi\mu r}. \tag{9}$$

There are many forces acting on particles moving in blood vessels, including hydrodynamic drag, inertia, buoyancy, gravity, and particle-particle interactions. However, only the major forces are considered: the hydrodynamic drag and magnetophoretic force. Our model ignores inertia, buoyancy, gravitational, and particle-particle interaction forces because they are several orders of magnitude weaker than the magnetic force.

Magnetic particles injected at far upstream of the occlusion enter the region of interest (ROI), i.e., the occluded region, in the form of a homogeneous suspension. When the magnetic career particles are transported in the vasculature, they simultaneously experience magnetic force, viscous drag force, gravitational (including buoyancy) forces, particle inertial effect, and thermal Brownian effects. The trajectory of a discrete phase particle is obtained by integrating the force balance on the particle. This force balance equates the particle inertia with the forces acting on the particle. Where additional acceleration force includes contribution from the drag force (FD), magnetic force (FM), buoyancy force (FG), Brownian force (FB) and thermos-phoretic force (FT) per unit particle mass. Note that the initial concentration is equal to 0.03 in the whole vessel.

The externally applied magnetic field strength and the electrical conductivity of the blood are two most important parameters for the FHD and MHD problems. In order to study the effect of both of this two parameters we introduce, the concepts blood viscosity. Normally, the red blood cells occupy 35% to 50% of the blood. Therefore deformability, orientation and aggregation of red blood cells result in shear-thinning viscosity of the blood. For non-Newtonian behavior of the blood, its viscosity becomes a function of shear rate. Therefore a relation between viscosity and shear rate is required. The Relation between shear stress and shear rate is:

$$\tau = \mu[\dot{\gamma}] \tag{10}$$

In equation 10, the shear stress tensor is given by:
$$\tau = \mu[\nabla V + (\nabla V)^{tr}] \tag{11}$$

And the shear rate is given by:
$$\dot{\gamma} = [\nabla V + (\nabla V)^{tr}] \tag{12}$$

And viscosity is given by the power law model as follow [12]:
$$\mu = m\dot{\gamma}^{n-1} \tag{13}$$

where values for m and n are given in Table 1. In our study if viscosity that is calculated from power law model (Eq. 13) becomes greater than μ_{Max}(0.02) or smaller than μ_{Min}(0.00309), the calculated values are replaced by maximum or minimum value. All other parameters are given in Table 1.

Table 1: Blood thermo-physical and magnetic Nano-particles properties

Parameters	Value	SI unit
ρ	800	$\frac{Kg}{m^3}$
χ	0.4,0.04,0.004	
r_P	$(1,0.1,0.01) \times 10^{-6}$	m
m	0.012	
n	0.8	
D	10^{-9}	$\frac{m^2}{s}$
μ_0	$4\pi \times 10^{-7}$	
μ	0.001	$\frac{N.s}{m^2}$
A	L/2	m
B	W+0.003	m
W	0.01	m
L	0.2	m

A finite volume code is developed and utilized. At the inlet to the vessel dimensionless concentration is equal to 1, see Figure 1. Also, at the exit of the vessel Neumann boundary condition is applied. Furthermore the upper and lower walls are insulated. In addition the diffusion coefficient (D) is equal to $1 \times 10^{-9} \frac{m^2}{s}$ [6]. A thin, straight wire carrying a current is placed along the x-axis, as shown in Figure 1. Evaluate the magnetic field at any internal points. Note that we have assumed that the leads to the ends of the magnet make call off contributions to the net magnetic field at any internal point.

RESULTS AND DISCUSSION

As investigated before [63] fish mortality during 24, 48, 72 and 96h of exposure were recorded. The results showed that fish mortality increased with increasing concentration and exposure time. After exposure to high concentrations (105 and 95 mg/L) fish were showed immediately some abnormal behaviors such as gill cover movements, abnormal swimming and jumping out of the water and their activity were reduced gradually and stayed at the floor of water in steady state, then came to surface of water and lost their balance finally died. The dead fish has a natural color. In control treatment, all fish showed normal behaviors and any signs of abnormal behavior were not observed. The maximum acceptable toxicant concentration (MATC) of silver nanoparticles for common carp at intervals of 24, 48, 72 and 96 hours was determined 7.95, 5.22, 3.06 and 1.13mg/L respectively. After 2 hours of reaction, nanoparticle absorption peak wavelength was detected at 406nm. This peak represents reduction of silver ions and forming the silver nanoparticles using extracts of seaweed *Sargassum angustifolium*. Therefore it is necessary that the toxicity of nanoparticles in order to have a better understanding of their effects on the aquatic environment that should be assessed separately in different species. In the present study the different species of fish, the synthesis method of examined nanoparticle was different compared with other studies, there it is expected that the results of the present study will be vary in toxicity with other studies. Figure 3 depicts the contour for B-field vector flow of 2000 nm magnetic particles with susceptibility (χ) of 0.004. The vessel width is equal to 1 mm and inlet velocity is 0.001 m/s. As shown, near the magnetic source, concentration of particles increase and particles create an obstacle in flow of blood. Ampacity and resistance of the standard copper wires used. The used diameter is 0.32 mm, area is 0.32 mm2, resistance is 212.9 (Ω/km), and current is 1.4 Ampere.

Figures 4 show the B-Y component for the inlet velocity equal to 1 mm/s. As shown by Fig 2 the Nano-particles shift towards the magnet (because of high magnetic force) as bio-fluid (blood) pass the magnet. It reduces the diameter of the channel and causes the blood velocity increases underneath of the particles. The magnetic field density and gradient produced by the optimum coil structure were sufficient for positioning micro particles, but not nanoparticles. To amplify the magnetic field to the extent required for nanoparticle positioning, soft iron cores were added to the design. Previous designs used linear systems [10-14], so the cores were not considered for use in the electromagnets because the cores make a magnetic field non-linear. In our design, however, because the effect of the force direction on particle trajectory is more important than the effect of the linearity of the force magnitude, the nonlinearity of the magnetic field is insignificant. As a result, it is possible to use cores inside the coils and amplify the magnetic field. However, the size and shape of the cores should be selected carefully such that the magnetic field intensity and gradient are both improved across the entire ROI defined for the actuator.
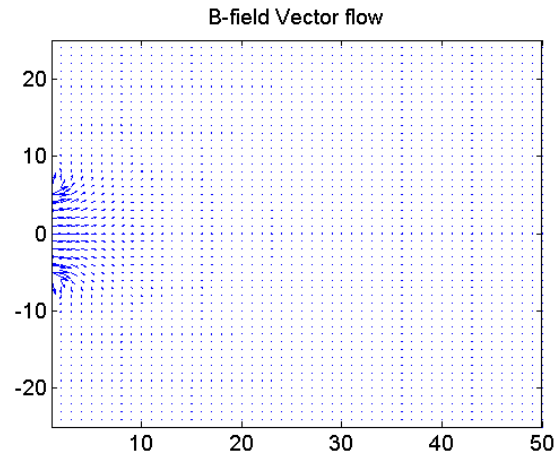
B-field Vector flow

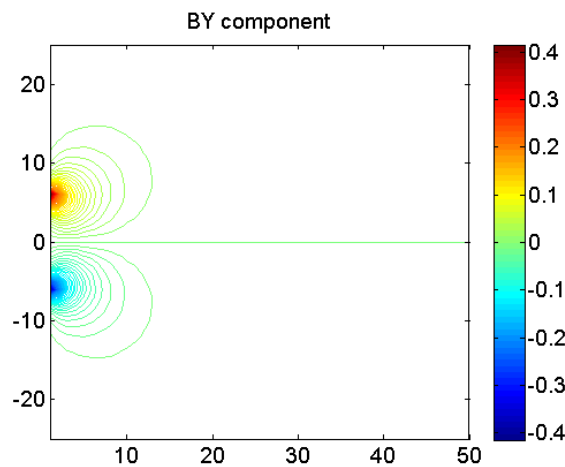**Fig. 3.Contour for B-field vector flow of 2000 nm magnetic particles**

BY component

Fig.4.B-Y component in 1 mm/s inlet velocity

The real picture of common carp (Cyprinuscarpio) is shown in figure 5. The common carp (Cyprinuscarpio) is a prevalent freshwater fish of eutrophic waters in lakes and large rivers in Europe and Asia. The wild populations are considered vulnerable to extinction, but the species has also been domesticated and introduced into environments worldwide, and is often considered a very destructive invasive species, being included in the List of the world's hundred worst invasive species. In Targeted Drug Delivery ,a procedure of transferring medicine particles to a patient , that increases the concentration of the medicine in diseased affected parts of the body relative to others.

Fig.5. Real picture of common carp (Cyprinuscarpio)

The Circulatory System in Cyprinuscarpio is shown in figure 6. The circulatory system of Cyprinuscarpio is included of both static and dynamic mechanisms. The dynamic part is the blood with all its constituent parts that flows continuously around the fish's body. The static parts are the heart, the veins and arteries leading to and from it and the capillaries that connect them. Normally between 3% and 8% of a Cyprinuscarpio's body weight is blood.
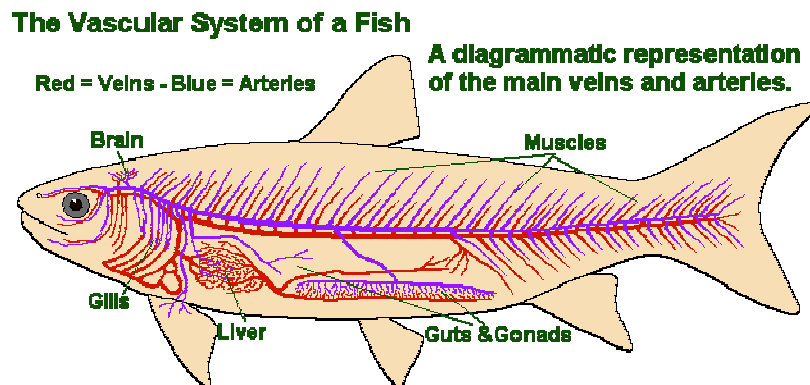

Fig. 6.Real picture of common carp (Cyprinuscarpio)

By adding nanoparticles in blood the effect of magnetic field can investigated. Many recent studies have been made on the nature of blood pathways through the gills of Cyprinuscarpio. Values for flow velocity and its pulsation in the afferent filament arteries of four goldfish averaged 0.65 ± 0.34 mm/s (S.D.) and 0.63 ±0.22 for arteries whose diameter range from 12-15 μm respectively. Corresponding values for the efferent arteries having diameters ranging from 15-47 μm were 0.63± 0.34 mm/s and 0.26 ± 0.20 mm/s respectively. The relatively large standard deviation in the flow velocities obtained from different fish is mainly attributable to variations in the depth of anaesthesia and perhaps the unnatural orientation of the fish. Flow velocities recorded were probably lower than those that occur under normal physiological conditions. The maximum flow velocity observed (i.e. about 1 mm/s in both the afferent and efferent filament arteries) may represent the actual flow velocity. This velocity is smaller than that measured in the micro vessels of frog lung. The flow velocity in the filament arteries is slightly lower than 1 mm/s at 18-20 °C and is more pulsatile in the afferent than in the efferent artery. Fish possess a two-chambered organ composed of one atrium and one ventricle. Blood is pumped from the ventricle through the conus arteriosus to the gills. Blood then moves on to the organs of the body, where nutrients, gases, and wastes are exchanged. The blood travels from the heart to the gills, and then directly to the body before returning to the atrium through the sinus venosus to be circulated again. The heart rates of fish fall within the wide range of 60-240 beats per minute, depending upon species and water temperature (slower at lower temperatures).
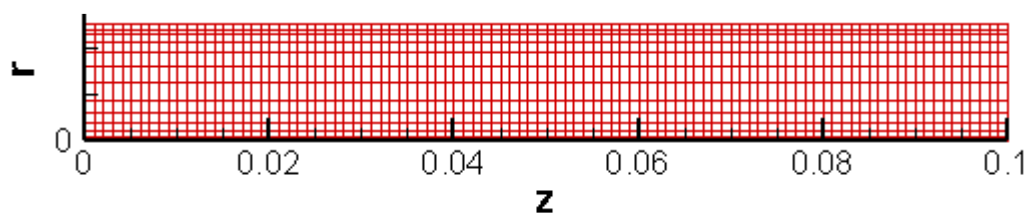

Fig. 7.Mesh of blood vessel

The mesh plot to solve problem is plotted in figure 7. When 3 μl of silver nanoparticles for drug and gene delivery is injected in the test section at a rate of 1 μl/s, the silver nanoparticles travels downstream in the form of streak-lines along the lower part of the tube with very little cross stream diffusion (for an average particle diameter of 10 nm, the silver nanoparticles diffusivity, as per the Stokes approximation, in distilled water is of the order of $10–11$ m^2/s). When no magnetic field is applied, the silver nanoparticles streak lines leave the test section, closely following the flow streamlines. However, as the bar magnet is applied (cf. Fig. 8) with a corner touching the outer wall of the tube, the silver nanoparticles forms a conical structure due to the action of the magnetic body force.

In the next simulation particles, distributed uniformly on the inlet surface, were released in the channel and their paths were captured for 2 seconds. The resultant particle trajectories are depicted in Fig. 9. Although most particles went to the correct outlet, some did not. This occurred because the initial position of some of the particles was far from the center of the inlet and they required a stronger magnetic field to attract them toward the correct outlet. Since the drag force in the blood flow direction is much greater than the magnetophoretic force for moving

nanoparticles in a blood vessel, the transfer of particles in the reverse direction of blood flow is practically impossible. Consequently, in our approach, the particles move along the vessels using the blood flow drag force and then the magnetic actuation system is implemented as a navigation system inside the vessel network. In this situation, the resistive drag force exerted on particles in vessel could be estimated as the opposing drag force on particles moving inside a stable fluid. Moreover, we defined the DCC approach, which has many advantages compared to the Helmholtz-Maxwell combination system. With the DCC approach, two coils are applied for each direction, and it is possible to make the system more compact, resulting in a stronger magnetic field and deeper penetration of magnetic gradient. Other advantages of the DCC approach include reduced cost and power consumption, as well as the capability of using coils with a core that improve the magnetophoretic force, making this system more desirable for nanoparticle steering.

The entire silver nanoparticles mass is transported by advection to the region near the dipole tip in 100 s (the supply streak lines are visible in Figs. 8 to Fig.10). The silver nanoparticles accumulation rate exceeds its wash away rate during this time and the size of the nanoparticle aggregate grows into a conical shape. Once fresh supply to the aggregate ceases, the advective and diffusive transport of the silver nanoparticles into the continually flowing host water stream leads to depletion in the silver nanoparticles aggregate. This phase is presented through the image sequences in Fig. 9.

Fig. 8 to 10 indicates how the axial velocity of fluid is influenced by the volume fraction density of the silver nanoparticles. One can see that, the axial velocity decreases by increasing the volume fraction density of the particles. The parabolic nature of the axial velocity is seen in the annular space between the artery and the catheter walls. So, the value of axial velocity is higher for a non-Newtonian fluid than that for a particle-fluid suspension model.

The effect of the volume fraction density of the particles on the pressure drop across the length of the time-variant overlapping Δp is displayed in Fig. 10. The variation of the pressure drop across the length of the time-variant overlapping Δp with volume flow rate for different values of the time is displayed in Fig. 8-10. At t = 0.1, we can explain that the pressure drop Δp increases as the r increases and the magnitude of the pressure drop Δp is higher in the case of non-uniform magnetic field. Finally, a careful investigation of this figure reveals that the relation between Δp and flow is found to be linear (the pressure drop Δp increase by increasing the flow rate) and the minimum pressure drop is achieved at zero flow rate. The simulation results were approved that this system could generate the necessary magnetic field for nano-particle propulsion. Moreover, it was accepted that there is a possibility to perform suitable control on particle trajectory. Since for moving nano-particle in blood vessel, the drag force in blood flow direction is much greater than the magneto-phoretic force, transferring the particles in reverse direction of the blood flow is practically impossible. For that reason, the particles are moving inside the vessels using the blood flow and then the magnetic actuation system is implemented as a navigation system inside the vessels network. In this situation, the exerted drag force on particles could be estimated by drag force on moving particle inside the stable fluid. Accordingly, the stable water was considered as fluid environment in our simulations. Moreover, for navigation method, constancy of the force and velocity in the entire particle trajectory is not essential and only the magnitude and direction of the force are important. Thus, nonlinearity of the magnetic field has no effective impact on the system performance.
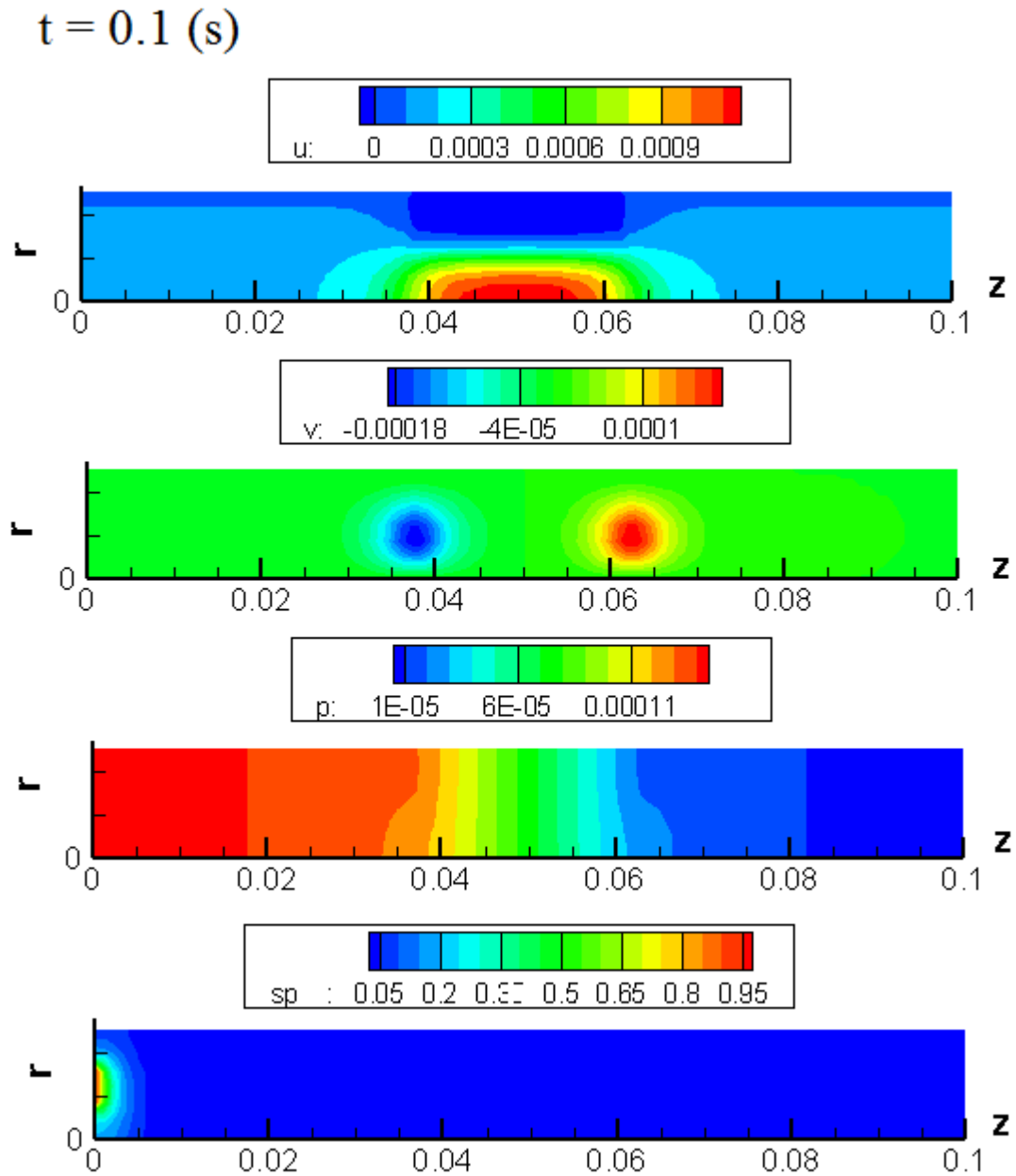
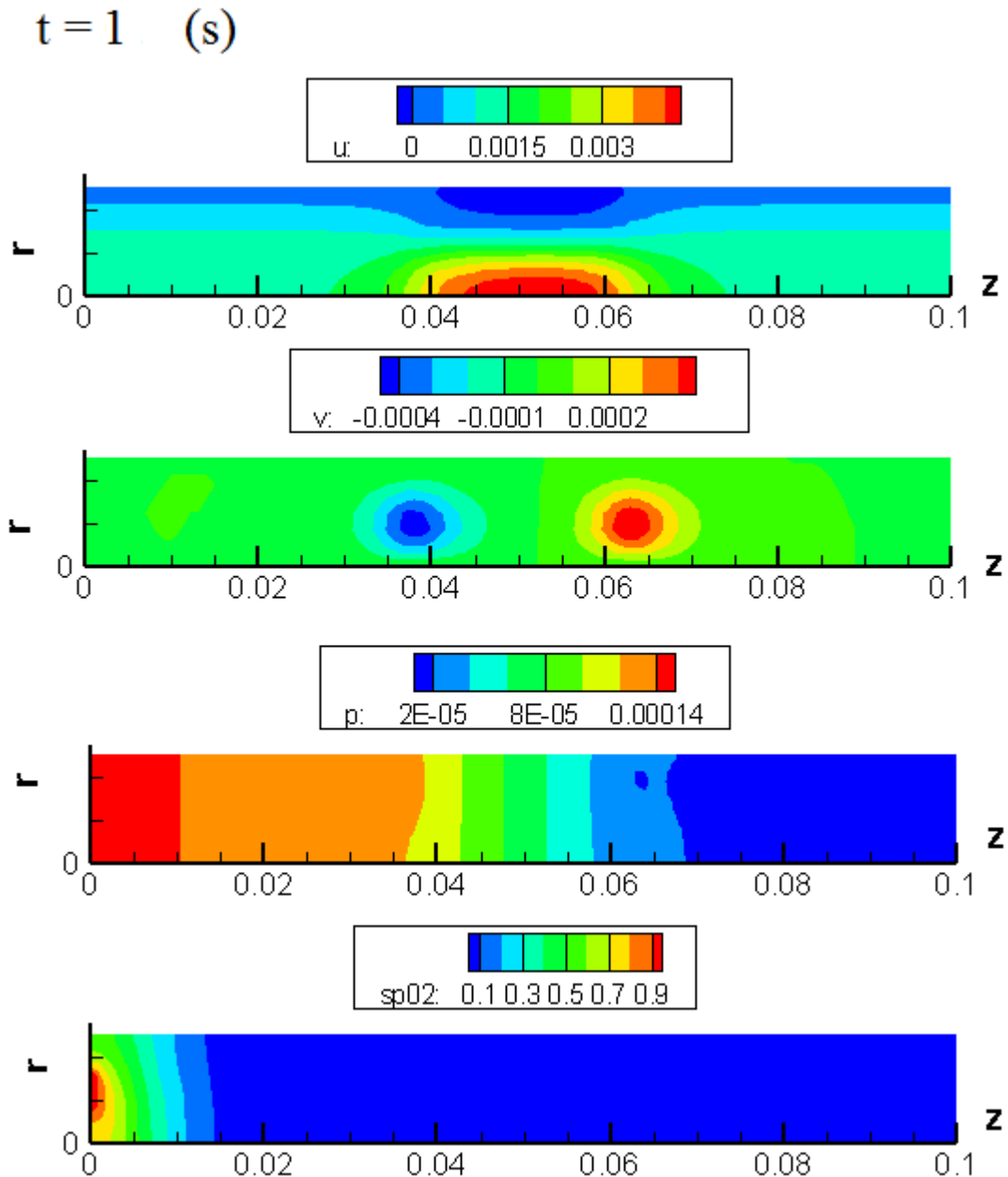**Fig. 8.Velocity component, pressure, and particle concentration at t = 0.1 (s)**

Fig. 9.Velocity component, pressure, and particle concentration at t = 1 (s)

The use of nanoparticles has been suggested for drug delivery to brain cells. Nanoparticles can cross into brain tissue and drugs encapsulated by these particles can be transferred to brain cells. Despite advances in the targeted delivery of magnetic particles to some organs (e.g., liver), transferring the particles to brain cells remains difficult due to the blood brain barrier, which prevents unrecognized particles from reaching brain cells; consequently, the delivery of therapeutic agents to specific regions of the brain represents a major challenge. Recently, localized hyperthermia has been used to overcome the blood brain barrier; it deactivates the blood brain barrier and allows the entry of micro-particles into the brain. Although this method is effective, the possibility of the influx of harmful particles into the brain with deactivation of the protective barrier increases and the applicability of this method is doubtful.
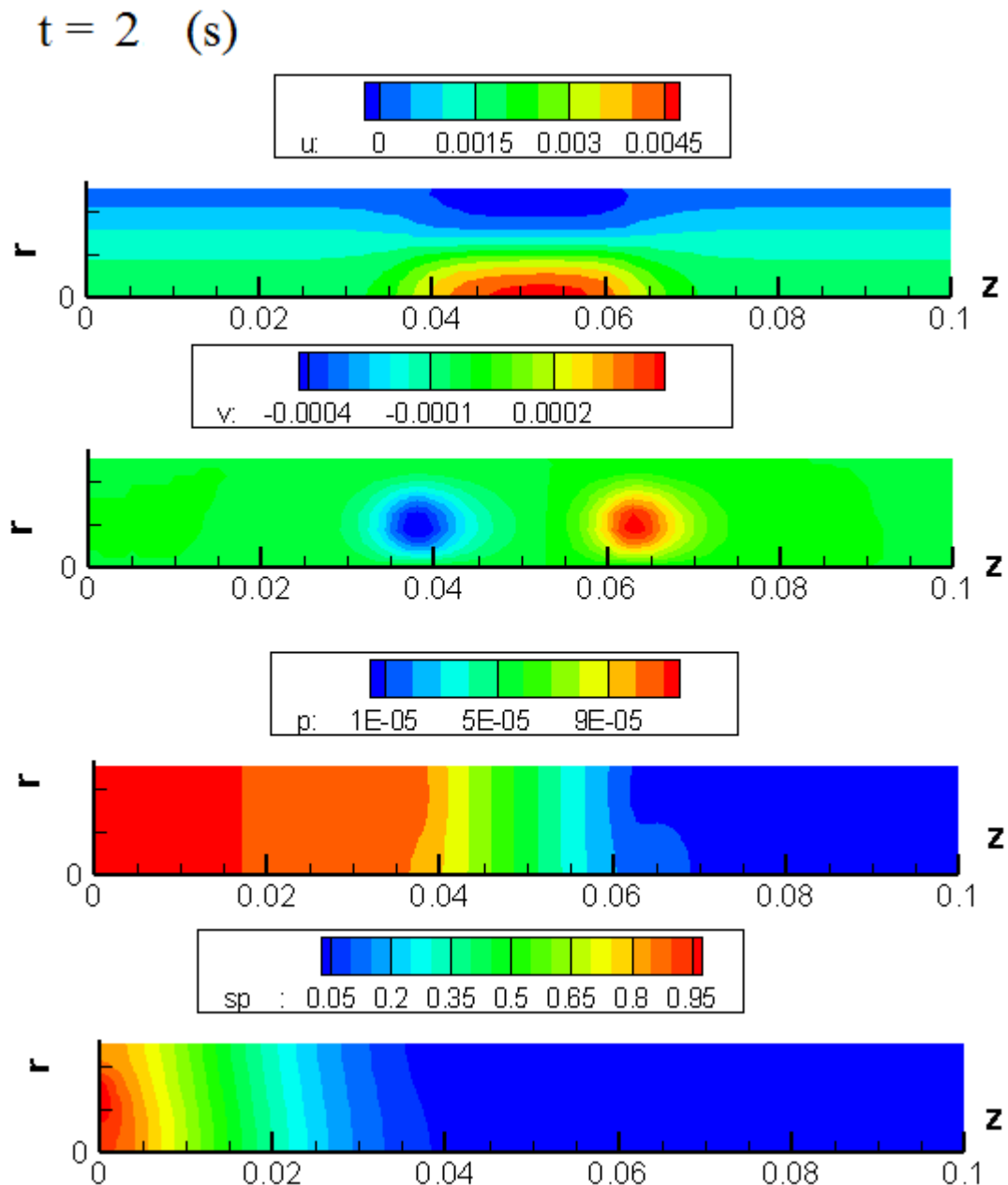
Fig. 10.Velocity component, pressure, and particle concentration at t = 2 (s)

CONCLUSION

Toxicity distribution in a sample blood vessel of a fish in common carp [42, 59] have been studied for silver nanoparticles synthesized using biological methods under application of magnetic field was studied. Beside the synthesis and fabrication of the nano-particles for targeting drug delivery here the propulsion system of these particles inside the blood vessels in the field of magnetic nano-particles drug delivery systems is investigated numerically. The main reason for these issues is the size of the nano-particles which need high power system for generating force and movement. In this paper, the feasibility of magnetic effects on silver nanoparticles for drug and gene delivery in Cyprinuscarpio was presented which could be used as a low cost and compact experimental setup for researches Configuration and dimensions of this system was chosen in such a way that could cover the size of the fish vessels, as an initial target of experiments. Moreover, to achieve realistic results, the currents and number of the electromagnet coils turns are considered realistic. Furthermore, the power suppliers could be unipolar which are in lower price compare to bipolar power supplier required for previous designs. This system needs more investigations for improvement. Finding the accurate relation between the current in the coils and the direction of the particle movement is an important research which will be presented in upcoming papers. Besides, simulation of the particle trajectory inside the realistic blood vessels and furthermore practical experiments are our future works.

REFERENCES

[1] M Y Abdollahzadeh Jamalabadi, *J Porous Media*, **2015**, 18(9),843-860.

[2] M Y Abdollahzadeh Jamalabadi;JH Park, *ThermSci*, **2014**,94-94

[3] M Y Abdollahzadeh Jamalabadi,*Int J OptAppl*, **2015**, 5 (5) , 161-167

[4] M Y Abdollahzadeh Jamalabadi*, ChemEng Res Des,* **2015**, 102 , 407-415

[5] M Y Abdollahzadeh Jamalabadi; JH Park, *World App Sci Journal*, **2014**,(4)32 , 672-677

[6] M Y Abdollahzadeh Jamalabadi;JH Park ; CY Lee, *entropy*, **2015**, 17 (2), 866-881

[7] AShahidian; MGhassemi; SKhorasanizade; MAbdollahzade; G Ahmadi, *IEEE Trans Magn,* **2009**,45 (6)2667-2670

[8] MY AbdollahzadehJamalabadi, *J. Marine Sci& App*, **2014**, 13(3) 281-290

[9] M Y Abdollahzadeh Jamalabadi; JH Park, *Int J.Sci Basic App Res Sci* 1 , **2014**, 421-427

[10] M Y Abdollahzadeh Jamalabadi; JH Park, O*pen J. Fluid Dyn*, **2014**,23 (4) 125-132

[11] MY AbdollahzadehJamalabadi;JHPark;MMRashidi;JM Chen, *J.Hydrod Ser. B,* **2016**

[12] M Y Abdollahzadeh Jamalabadi,*Front Heat Mass Trans*, **2015**,6,013007

[13] M.Y. AbdollahzadehJamalabadi, *J. Fuel Cell Sci. Technol*, **2013**, 10(5) ,1039

[14] M Y Abdollahzadeh Jamalabadi;JHPark; CY Lee, *ThermSci*, **2014**,124-124

[15] M Jamalabadi; P Hooshmand; BKhezri ; ARadmanesh, *IndJ sci Res* ,**2014**, 74-81

[16] M Y Abdollahzadeh Jamalabadi, Mul Model Mat Struc,**2016**

[17] M.Y. AbdollahzadehJamalabadi, J.H.Park,C.Y. Lee, *International Journal of Applied Environmental Sciences*, **2014**,9 (4)1769-1781

[18] M Y Abdollahzadeh Jamalabadi, *World App. Sci. J.***2014**,32 (4) 667-671

[19] M Y Abdollahzadeh Jamalabadi, *Mid-East J. Sci Res* **2014**, 22 (4)561-574

[20] M Y Abdollahzadeh Jamalabadi, *Mat .Perf.Char*, **2015** 20140062

[21] MSShadloo;RPoultangari; MY AbdollahzadehJamalabadi, MM Rashidi , *Energy Conversion and Management*, 96 (2015) 418-429

[22] M Y Abdollahzadeh Jamalabadi; MGhasemi; MH Hamedi ,*Int J Numer Meth Heat Fluid Flow* 23 () 4 (2013) 649-661

[23] M Y Abdollahzadeh Jamalabadi, In*t J Ener Mat ChemPro* ,**2016** 15, DOI:10.1615/ *Int J Energetic Materials Chem Prop*.**2015** 014428

[24] M Y Abdollahzadeh Jamalabadi, *Noise and Vibration Worldwide* 45 (8)(**2014**) 21-27

[25] M Y Abdollahzadeh Jamalabadi, J.King *Saud UnivEngSci* 26 (2)(**2014**) 159-167

[26] M Y Abdollahzadeh Jamalabadi ; M Ghasemi ;MH Hamedi, Proc Inst MechEng, Part C, *J. MechEngSci* 226 (**2012**) 1302-1308

[27] M.Y. AbdollahzadehJamalabadi, *Int J EnerEng*, **2015**, 5(1) 1-8

[28] M.Y. AbdollahzadehJamalabadi, *Int J Mult Res Dev*, (1) 5 (**2014**) 1-4

[29] S Dousti; J Cao; A Younan; P Allaire; T Dimond*, J. tribology* , **2012**,134 (3), 031704.

[30] SDousti; JA Kaplan, F He; PEAllaire, ASME *TurbExpConf* , **2013**.

[31] F He; PE Allaire; S Dousti; A Untaroiu , *ASME IntMechEng Cong Exp,* **2013**.

[32] SDousti; RLFittro, *ASME TurbExpConf* , **2015**.

[33] ESarshari; N Vasegh;M. Khaghani; SDousti, *ASME IntMechEng Cong Exp*, **2013**.

[34] SDousti; TW Dimond; PEAllaire, HE Wood, *ASME IntMechEng Cong Exp*, **2013**.

[35] SDousti;MAJalali, *J. App Mech*, **2013**, 80 (1), 011019.

[36] YG Sun; B Mayers; YN Xia *NanoLett* ,**2003**, 3, 675–679.

[37] V Venkatpurwar; V Pokharkar, *Materials Letters* ,**2011,**65, 999–1002.

[38] R Patakfalvi;Dekany, *Colloid*PolymSci,**2010**, 280, 461–470.

[39] P Kumar;Senthamil SS; A Lakshmi Prabha; K Prem Kumar;RS Ganeshkumar; M Govindaraju,.*Nano Biomed* Eng, **2012,**4, 2-16.

[40] P Mansuya; P Aruna; S Sridhar; JSKumar; S Babu, *Journal of. Exp. Sci*,**2010**,1, 23-26.

[41] K Fent, *Ecotoxicology of Engineered Nanoparticles* ,**2010**, 183-205.

[42] M Alishahi; M Mesbah; M Ghorbanpoor,*IranianJ Veterinary Res*,**2011**, 7,36-41.

[43] PV Asharani; YL Wu; Z Gong; S Valiyaveettil, *Nanotechnology* ,**2008**, 19, 1–8.

[44] K Bilberg; MB Hovgaard; F Besenbacher; EBaatrup*, J Toxicology* ,**2012**,293784,1-9.

[45] K Bilberg, H Malte, T Wang, E Baatrup, *Aquatic Toxicology* ,**2012**, 96,159-165.

[46] G Singaravelu; JS Arockiamary; KV Ganesh; K Govindaraju,*Colloids Surf. Biointerfaces*,**2007**,57, 97-101.

[47] P Jegadeeswaran; R Shivaraj; R Venckatesh,*Digest J Nanomaterials Biostructures* ,**2012**,7, 991 – 998.

[48] QA Pankhurst; NK T Thanh; SK Jones; and J Dobson, *J. Phys. D: Appl. Phys*., **2003**, 36, 13, 167–181.

[49] L Johannsen; J O Blanchette, *Adv. Drug Deliv,***2004**, 56, 1649–1659.

[50] M E Davis; Z Chen; D M Shin, *Nat. Rev. Drug. Discov*,**2008**, 7, 771–782.

[51] M Arruebo; R Fernandez-Pacheco; M R Ibarra; J Santamaria, *Nano Today*,**2007**, 2, 22-32.

[52] C Alexiou; R Jurgons; C Seliger; O Brunke; H Iro; S Odenbach, ,*Anticancer Res*,**2007**, 27, 4A, 2019–2022

[53] S I Takeda; F Mishima; S Fujimoto; Y Izumi; S Nishijima, *J Magn. Magn. Mater*,**2006**,311, 367-371.

[54] K B Yesin; K lmers; B J Nelson; *Int. J. Robot. Res*,**2006**, 25, 527-536

[55] J J Abbott; O Ergeneman; M P Kummer; A M Hirt; B J Nelson, *IEEE Trans. Robot*,**2007**, 23, 1247-1252

[56] C Alexiou; D Diehl; P Henninger; H Iro; R Rockelein; W Schmidt; H Weber, *IEEE Trans. Appl. Supercond,***2006**, 16, 1527–1530

[57] X Han; Q Cao; and L Li, *IEEE Trans. Appl. Supercond*, **2012**, 22, 3, 4401404– 4401404

[58] J-B Mathieu; S Martel, *Biomed Microdevices*,**2007**,9, 801–808

[59] S Martel; O Felfoul; J-B Mathieu; A Chanu; S Tamaz; M Mohammadi; M Mankiewicz; N Tabatabaei, *Int. J. Rob. Res,***2009**, 28, 9, 1169–1182

[60] H Choi; J Choi; G Jang; J Park; S Park, *Smart Mater. Struct*,**2009**, 18, 5, 055007

[61] S Jeon; G Jang; H Choi; S Park, *IEEE Trans. Magn*,**2010**,46, 6, 1943–1946

[62] H Choi; K Cha; J Choi; S Jeong; S Jeon; G Jang; J Park; S Park, *Sens. Actua. A: Phys*,**2010**, 163, 1, 410–417

[63] M Y AbdollahzadehJamalabadi et al *J. Chem. Pharm. Res*., **2015**, 7(11):91-98